Energy Density Functional Study of Nuclear Matrix Elements for Neutrinoless $\beta\beta$ Decay

Tomás R. Rodríguez[1,2,3] and Gabriel Martínez-Pinedo[1]

[1]GSI Helmholtzzentrum für Schwerionenforschung, D-64259 Darmstadt, Germany
[2]Departamento de Física Teórica, Universidad Autónoma de Madrid, E-28049 Madrid, Spain
[3]CEA, Irfu, SPhN, Centre de Saclay, F-911191 Gif-sur-Yvette, France

(Received 31 August 2010; published 15 December 2010)

We present an extensive study of nuclear matrix elements (NME) for the neutrinoless double-beta decay of the nuclei ^{48}Ca, ^{76}Ge, ^{82}Se, ^{96}Zr, ^{100}Mo, ^{116}Cd, ^{124}Sn, ^{128}Te, ^{130}Te, ^{136}Xe, and ^{150}Nd based on state-of-the-art energy density functional methods using the Gogny D1S functional. Beyond-mean-field effects are included within the generating coordinate method with particle number and angular momentum projection for both initial and final ground states. We obtain a rather constant value for the NMEs around 4.7 with the exception of ^{48}Ca and ^{150}Nd, where smaller values are found. We analyze the role of deformation and pairing in the evaluation of the NME and present detailed results for the decay of ^{150}Nd.

DOI: 10.1103/PhysRevLett.105.252503 PACS numbers: 21.60.Jz, 23.40.Hc

Double-beta decay is an extremely rare process where an even-even nucleus decays into the even-even neighbor bypassing the energetically forbidden odd-odd intermediate isobar. Along the nuclear chart, there are only few candidates, all found in the valley of stability [1]. The double-beta decay where two electrons and two neutrinos are emitted in the final state ($2\nu\beta\beta$) has been observed experimentally in several isotopes with half-lives $\sim 10^{19-21}$ yr. This process conserves the leptonic number and is compatible with Majorana or Dirac neutrinos. There is also a second mode without neutrino emission ($0\nu\beta\beta$) that is possible only if the neutrinos are massive Majorana particles and is related to the absolute mass scale of these elementary particles [1]. Other than one controversial claim [2], $0\nu\beta\beta$ decay has not been detected and is currently the main goal of several projects worldwide [3]. The half-life of this process between 0^+ states for mother and granddaughter nuclei can be written as [1]

$$[T^{0\nu}_{1/2}(0^+ \to 0^+)]^{-1} = G_{01}|M^{0\nu}|^2\left(\frac{\langle m_{\beta\beta}\rangle}{m_e}\right)^2, \qquad (1)$$

where $\langle m_{\beta\beta}\rangle$ is the effective Majorana neutrino mass, m_e is the electron mass, G_{01} is a kinematical phase space factor, and, finally, $M^{0\nu}$ is the nuclear matrix element (NME). Equation (1) shows that a precise determination of the effective neutrino mass requires, apart from the experimental measurement of the $0\nu\beta\beta$ half-life, a reliable calculation of the NME. Thus far, several nuclear structure methods have been employed. The most used among them are the interacting shell model (ISM) [4,5], proton-neutron quasirandom phase approximation (QRPA) [6–9], and, more recently, projected Hartree-Fock-Bogoliubov (PHFB) in limited configuration spaces and using schematic pairing plus quadrupole interactions [10,11] and interacting boson model (IBM) [12].

In this Letter, we present major improvements with respect to previous PHFB calculations [10,11]: we use state-of-the-art density functional methods based on the well-established Gogny D1S functional [13] and a much larger single particle basis (11 major oscillator shells); we perform particle number and angular momentum projection (PNAMP) for both mother and granddaughter nuclei; and include configuration mixing within the generating coordinate method (GCM) framework [14,15]. All these developments have been shown to be necessary for a unified description of nuclear structure [14]. In particular, particle number projection before variation is fundamental for a correct treatment of pairing correlations [15] that play a very important role in $0\nu\beta\beta$ decay [4].

The $0\nu\beta\beta$ NME can be separated into three terms: Fermi (F), Gamow-Teller (GT), and tensor (T) [1]:

$$M^{0\nu} = -\left(\frac{g_V}{g_A}\right)^2 M^{0\nu}_F + M^{0\nu}_{\rm GT} - M^{0\nu}_T, \qquad (2)$$

with $g_V = 1$ and $g_A = 1.25$. The tensor term is small according to the ISM and QRPA calculations [5,8] and will be neglected in this work. We use the closure approximation [1] to sum over intermediate states in the odd-odd nucleus as currently it is not possible to compute odd-odd nuclei using beyond-mean-field methods: symmetry restoration methods including blocking effects have not been fully developed so far. Therefore, a calculation of the $2\nu\beta\beta$ mode cannot be performed as the closure approximation is not valid in this process. The different terms in Eq. (2) can be expressed as the expectation value of a two-body operator between the initial and final states; i.e., $M^{0\nu}_{F/\rm GT} = \langle 0^+_f|\hat{M}^{0\nu\beta\beta}_{F/\rm GT}|0^+_i\rangle$. Detailed expressions for $\hat{M}^{0\nu\beta\beta}_{F/\rm GT}$ can be found in Ref. [5]. We have included high order currents [6], nucleon finite size corrections [6], and radial short-range correlations treated within the unitary correlator method (UCOM) [8,16]. In the GCM + PNAMP approach (GCM from now on), the initial (i) and final (f) many-body wave functions are found as linear combinations of particle number N, Z, and angular momentum $I = 0$ projected

wave functions with different intrinsic quadrupole deformations β:

$$|0^+\rangle = \sum_\beta g_\beta P^{I=0} P^N P^Z |\Phi_\beta\rangle, \quad (3)$$

where $P^{I=0}$, P^N, P^Z are the corresponding angular momentum ($I = 0$) and particle number projectors [17]. The intrinsic axial symmetric Hartree-Fock-Bogoliubov wave functions $|\Phi_\beta\rangle$ are solutions to the variation after particle number projection equations constrained to a given value of the axial quadrupole deformation, β [15,18]. Therefore, intrinsic deformation of the system is naturally included in the formalism and pairing correlations properly taken into account. Finally, the coefficients g_β are found by solving the Hill-Wheeler-Griffin equation [17,19]. First, for each nucleus we transform the nonorthogonal set of wave functions $\{P^{I=0}P^NP^Z|\Phi_\beta\rangle\}$ into an orthonormal one $\{|\Lambda\rangle = \sum_\beta (u_{\Lambda,\beta}/\sqrt{n_\Lambda}) P^{I=0}P^NP^Z|\Phi_\beta\rangle\}$ by diagonalizing the norm overlap matrix, $\sum_{\beta'}\langle\Phi_\beta|P^{I=0}P^NP^Z|\Phi_{\beta'}\rangle u_{\Lambda,\beta'} = n_\Lambda u_{\Lambda,\beta}$. In this basis, the Hill-Wheeler-Griffin equation reads: $\sum_{\Lambda'}\varepsilon_{\Lambda\Lambda'}G^a_{\Lambda'} = E^a G^a_\Lambda$, where $\varepsilon_{\Lambda\Lambda'}$ are the so-called energy kernel [15,19]. Finally, the coefficients for the lowest eigenvalue are used to compute both the so-called collective wave functions $F(\beta) = \sum_\Lambda G^0_\Lambda u_{\Lambda,\beta}$—probability distribution for the state to have a given deformation—and the NME:

$$M^{0\nu}_{F/\mathrm{GT}} = \sum_{\Lambda_i\Lambda_f}\sum_{\beta_i\beta_f}\left(\frac{u^*_{\Lambda_f,\beta_f}}{\sqrt{n_{\Lambda_f}}}\right) G^{0*}_{\Lambda_f}\langle\Phi_{\beta_f}| \times |P^{N_f}P^{Z_f}\hat{M}^{0\nu}_{F/\mathrm{GT}}P^{I=0}P^{N_i}P^{Z_i}|\Phi_{\beta_i}\rangle G^0_{\Lambda_i}\left(\frac{u_{\Lambda_i,\beta_i}}{\sqrt{n_{\Lambda_i}}}\right). \quad (4)$$

Particle number conservation together with using large and identical configuration spaces for protons and neutrons guarantees that Ikeda's sum rule is fulfilled. Additionally, to our knowledge, this is the first implementation of the GCM method for calculating transitions between different nuclei including particle number symmetry restoration in both the initial and final states.

We now present our results for the $0\nu\beta\beta$ NME, discussing in detail the decay of ^{150}Nd. To check the reliability of the method for describing properties of the initial and final nuclei, we show in Fig. 1 a comparison between the experimental and theoretical ground state bands for ^{150}Nd and ^{150}Sm. We observe a rather good agreement for both excitation energies and $B(E2)$ transition probabilities, with the theoretical results predicting a slightly larger rotational (collective) character than the experiment. The computed double-beta decay Q value is 2.99 MeV while the experimental value is 3.37 MeV. The inset of Fig. 1 shows the probability distribution for the mother and granddaughter 0^+_1 states to have a given intrinsic quadrupole deformation β. Both ^{150}Nd and ^{150}Sm have well deformed prolate ground states with $\beta \approx +0.40$ and $\beta \approx +0.25$, respectively. These values are compatible

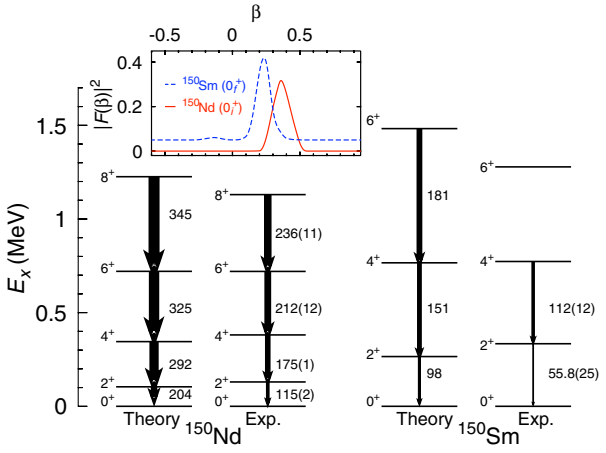

FIG. 1 (color online). Comparison between theoretical and experimental ground state bands for ^{150}Nd and ^{150}Sm. Inset: Collective wave functions of the ground states as a function of the intrinsic deformation. The values for ^{150}Sm have been shifted up by 0.05.

with the rotational bands shown in the figure. Equation (4), shows that the $0\nu\beta\beta$ NME can be expressed as a sum of matrix elements between states of different intrinsic quadrupole deformation for the initial and final nuclei. Consequently, the matrix element

$$\frac{\langle\Phi_{\beta_f}|P^{N_f}P^{Z_f}\hat{M}^{0\nu\beta\beta}_{F/\mathrm{GT}}P^{I=0}P^{N_i}P^{Z_i}|\Phi_{\beta_i}\rangle}{\sqrt{\langle\Phi_{\beta_f}|P^{N_f}P^{Z_f}P^{I=0}|\Phi_{\beta_f}\rangle\langle\Phi_{\beta_i}|P^{N_i}P^{Z_i}P^{I=0}|\Phi_{\beta_i}\rangle}}$$

provides explicitly the strength of the $0\nu\beta\beta$ operators as a function of the deformation of the nuclei involved in the decay. In Fig. 2(a) we show these matrix elements for the GT component (the Fermi part gives a similar pattern and it is not shown). The strength is concentrated rather symmetrically in the diagonal part of the figure, implying that the decay between states with different initial and final deformation is hindered. Moreover, spherical configurations are the most preferred to decay. Nevertheless, Fig. 2(a) also shows an interval of deformation close to the spherical configuration where non-negligible off-diagonal matrix elements (greater that 0.5) are obtained ($\beta \in [-0.2, +0.2]$). The absolute maximum is found at $(+0.03, 0)$ with additional local maxima, for example, at $(+0.52, +0.52)$. These results are in agreement with ISM and PHFB calculations that have shown a significant decrease of the NME with increasing difference in quadrupole deformation between initial and final states [10,20]. This trend has also been observed in $2\nu\beta\beta$ QRPA calculations [21]. The final value of the NME is determined by weighting the strength of the transition operator with the wave functions of the initial and final states which selects the relevant region of deformation. This area is marked by a shaded circle in Fig. 2(a) showing that in this case both the difference in deformation and the absence of shape mixing inhibit the transition. The final result for the NME is $M^{0\nu} = 1.71$ with 1.28 and 0.43 coming from

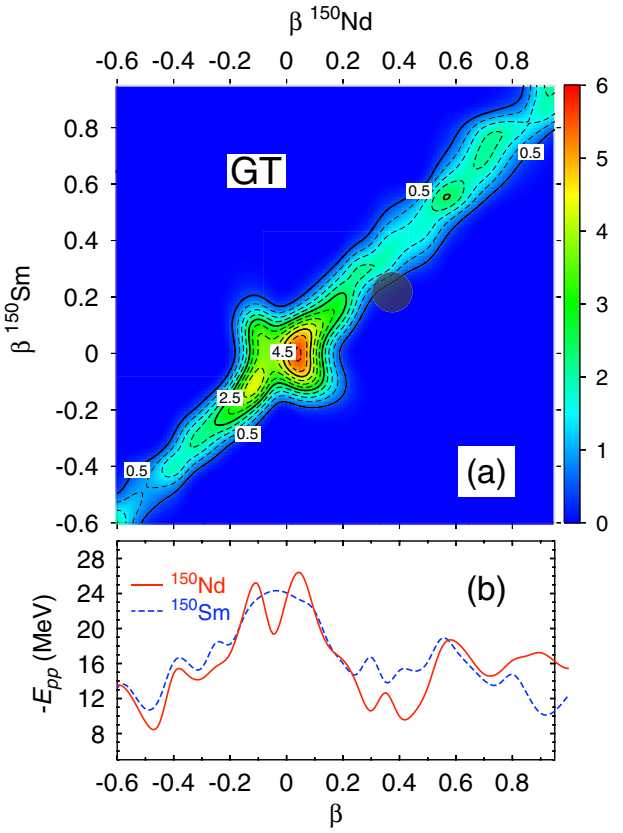

FIG. 2 (color online). (a) Strength of the GT operator as a function of the intrinsic deformation of the mother and granddaughter nuclei. Shaded area corresponds to the maximum probability for finding the mother and granddaughter states. (b) Pairing energies as a function of the intrinsic deformation.

Gamow-Teller and Fermi components, respectively. In order to shed additional light on the structure of the strength, we show in Fig. 2(b) the pairing energy $-E_{pp}$ of the nuclei involved in the decay. This energy is defined as the pairing tensor part [14,17] within the PNAMP approach. We find a strong correlation between the structure of the NME and $-E_{pp}$, both having maxima at similar values of the deformation for mother and granddaughter nuclei. This result is also in agreement with ISM and QRPA calculations where the largest values for the NME are obtained with well paired wave functions with large zero seniority components in the spherical basis [4,7].

We now present the values of the NME [Eq. (4)] computed for several double-beta emitters and compare with the ones calculated with other methods that use similar assumptions concerning the neutrino potentials. In Fig. 3 we observe that the NMEs are rather constant around an averaged value of 4.7 for the decay of ^{76}Ge, ^{82}Se, ^{96}Zr, ^{100}Mo, ^{116}Cd, ^{124}Sn, ^{128}Te, ^{130}Te, and ^{136}Xe, being ^{96}Zr the one with the largest value. In these nuclei, the differences in deformation between the initial and final states are not very significant and also the structure and absolute values of the transition strength are quite similar. There are two exceptions to this general trend, namely, ^{48}Ca and ^{150}Nd,

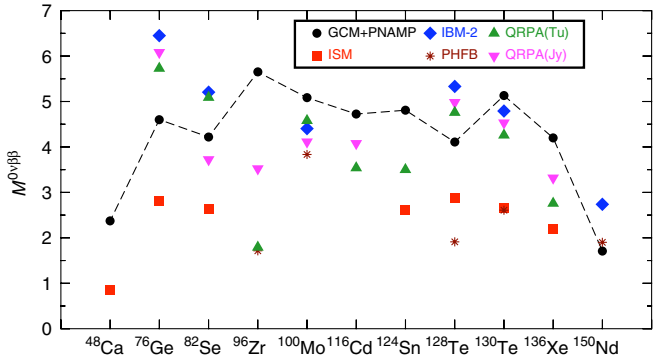

FIG. 3 (color online). Nuclear matrix elements calculated for different methods (ISM [5,22], QRPA(Jy) [8], QRPA(Tu) [7], IBM-2 [12], PHFB [10]) with UCOM short-range correlations. QRPA values are calculated with $g_A = 1.25$ and IBM-2 and PHFB results are multiplied by 1.18 to account for the difference between Jastrow and UCOM [29].

where the NME is significantly smaller. In the latter, the difference between deformation of the mother and granddaughter is remarkable (inset Fig. 1), and this is precisely the main source of suppression of the NME. On the other hand, due to the double magic character of ^{48}Ca, this nucleus has the smallest value for the pairing energy and transition strength among the nuclei studied in this work. Concerning the NME's obtained by other methods, we attribute first the small NMEs obtained by PHFB to the reduced configuration space used and the lack of particle number restoration and shape mixing in those calculations. We also show that the lowest NMEs are obtained within the ISM, a rather constant value around 2.5 except for ^{48}Ca. We expect that enlarging the model space used in the ISM calculations will enhance the values of their NMEs [4,9,22]. Considering higher seniority components in our method by including quasiparticle excitations in the intrinsic wave functions may reduce our values slightly. Some differences are also found between the GCM and QRPA values. The main differences between these approaches are the assumption of spherical symmetry in QRPA, the absence of quasiparticle excitations in the GCM approach, and the much larger—and no core—single particle basis used in GCM. Furthermore, neither triaxial, mirror, nor time reversal symmetry breaking effects are included in our GCM calculations because they are beyond current computational capabilities. We expect that the inclusion of these degrees of freedom will not significantly change the structure of the ground states as the nuclei studied here are either spherical or well deformed. To validate our approach we have computed the total GT strengths $S_{+(-)}$ for the decay of granddaughter (mother) nuclei defined, for example, in Ref. [23]. In Table I, we compare the calculated $S_{+(-)}$ with the experimental values measured in charge exchange reactions. As in QRPA and ISM calculations, a quenching factor of $(0.74)^2$ has been introduced [21,23]. Finally, we evaluate the half-life of each nuclei based on the NME calculated with the GCM method. In Table I, we show

TABLE I. Difference between theoretical and experimental Q values, total GT strength for granddaughter (mother) S_+ (S_-), NME, and predicted half-lives for several $0\nu\beta\beta$ decaying nuclei assuming $\langle m_{\beta\beta}\rangle = 0.5$ eV.

A	$Q_{\text{theo}} - Q_{\text{expt}}$ (MeV)	S_+	S_-	$M^{0\nu}$	$T_{1/2}$ ($\times 10^{23}$ yr)
48	0.265	1.99	13.55	2.37	28.5
		(1.9 ± 0.5 [24])	(14.4 ± 2.2 [24])		
76	0.271	1.49	20.97	4.60	76.9
		(1.45 ± 0.07 [25])	(19.89 [26])		
82	−0.366	1.24	23.56	4.22	20.8
			(21.91 [26])		
96	2.580	2.56	27.63	5.65	5.48
		(0.29 ± 0.08 [27])			
100	1.879	2.48	27.87	5.08	8.64
			(26.69 [26])		
116	1.365	2.61	34.30	4.72	9.24
		$(1.09^{+0.13}_{-0.57}$ [28])	(32.70 [26])		
124	−0.830	1.63	40.65	4.81	16.2
128	−0.564	1.45	40.48	4.11	343.1
			(40.08 [26])		
130	−0.348	1.19	43.57	5.13	8.84
			(45.90 [26])		
136	−1.027	0.96	46.71	4.20	12.7
150	−0.380	1.45	50.32	1.71	16.5

the difference between the calculated and experimental Q values and we observe an excellent agreement in most of the cases except for ^{96}Zr and ^{100}Mo, where an overbinding of ^{96}Mo and ^{100}Ru isotopes gives such differences. These are precisely the decays with largest NME and smallest half-lives predicted by our calculations.

In summary, we have presented the first calculations of $0\nu\beta\beta$ decay within the energy density functional framework including beyond-mean-field effects. We have analyzed the role of the intrinsic quadrupole deformation and pairing content of the nuclei involved in this process. Decays between spherical initial and final shapes are found to be favored while large differences in deformation significantly hinder the transition probability. Our calculations constitute the first consistent evaluation of the $0\nu\beta\beta$ decay of ^{150}Nd.

We thank A. Poves, J. Menéndez, J. L. Egido, K. Langanke, T. Duguet, and F. Nowacki for fruitful discussions. T. R. R. is supported by the Programa de Ayudas para Estancias de Movilidad Posdoctoral 2008 and FPA2009-13377-C02-01 (MICINN). G. M. P. is partly supported by the DFG through Contract No. SFB 634, by the ExtreMe Matter Institute EMMI and by the Helmholtz International Center for FAIR.

[1] F. T. Avignone, S. R. Elliott, and J. Engel, Rev. Mod. Phys. **80**, 481 (2008).
[2] H. V. Klapdor-Kleingrothaus *et al.*, Phys. Lett. B **586**, 198 (2004).
[3] H. Ejiri, Prog. Part. Nucl. Phys. **64**, 249 (2010).
[4] E. Caurier *et al.*, Phys. Rev. Lett. **100**, 052503 (2008).
[5] J. Menendez *et al.*, Nucl. Phys. **A818**, 139 (2009).
[6] F. Simkovic *et al.*, Phys. Rev. C **60**, 055502 (1999).
[7] F. Simkovic *et al.*, Phys. Rev. C **77**, 045503 (2008).
[8] M. Kortelainen and J. Suhonen, Phys. Rev. C **75**, 051303 (2007).
[9] J. Suhonen and O. Civitarese, Nucl. Phys. **A847**, 207 (2010).
[10] K. Chaturvedi *et al.*, Phys. Rev. C **78**, 054302 (2008).
[11] P. K. Rath *et al.*, Phys. Rev. C **80**, 044303 (2009).
[12] J. Barea and F. Iachello, Phys. Rev. C **79**, 044301 (2009).
[13] J. F. Berger, M. Girod, and D. Gogny, Nucl. Phys. **A428**, 23 (1984).
[14] M. Bender, P.-H. Heenen, and P.-G. Reinhard, Rev. Mod. Phys. **75**, 121 (2003).
[15] T. R. Rodríguez and J. L. Egido, Phys. Rev. Lett. **99**, 062501 (2007).
[16] H. Feldmeier *et al.*, Nucl. Phys. **A632**, 61 (1998).
[17] P. Ring and P. Schuck, *The Nuclear Many Body Problem* (Springer-Verlag, Berlin, 1980).
[18] M. Anguiano, J. L. Egido, and L. M. Robledo, Nucl. Phys. **A696**, 467 (2001).
[19] R. Rodríguez-Guzmán, J. L. Egido, and L. M. Robledo, Nucl. Phys. **A709**, 201 (2002).
[20] J. Menendez *et al.*, arXiv:0809.2183.
[21] R. Álvarez-Rodríguez *et al.*, Phys. Rev. C **70**, 064309 (2004).
[22] J. Menendez *et al.*, Phys. Rev. C **80**, 048501 (2009).
[23] E. Caurier *et al.*, Rev. Mod. Phys. **77**, 427 (2005).
[24] K. Yako *et al.*, Phys. Rev. Lett. **103**, 012503 (2009).
[25] R. L. Helmer *et al.*, Phys. Rev. C **55**, 2802 (1997).
[26] R. Madey *et al.*, Phys. Rev. C **40**, 540 (1989).
[27] H. Dohmann *et al.*, Phys. Rev. C **78**, 041602(R) (2008).
[28] S. Rakers *et al.*, Phys. Rev. C **71**, 054313 (2005).
[29] A. Poves (private communication).